

CHEMISTRY

A European Journal

A Journal of



Accepted Article

Title: Generation of Stable Ruthenium(IV)-Ketimido Complexes via Oxidative Addition of Oxime Esters to Ruthenium(II): Reactivity Studies Based on Electronic Properties of the Ru-N Bond

Authors: Takuya Shimbayashi, Kazuhiro Okamoto, and Kouichi Ohe

This manuscript has been accepted after peer review and appears as an Accepted Article online prior to editing, proofing, and formal publication of the final Version of Record (VoR). This work is currently citable by using the Digital Object Identifier (DOI) given below. The VoR will be published online in Early View as soon as possible and may be different to this Accepted Article as a result of editing. Readers should obtain the VoR from the journal website shown below when it is published to ensure accuracy of information. The authors are responsible for the content of this Accepted Article.

To be cited as: *Chem. Eur. J.* 10.1002/chem.201704102

Link to VoR: <http://dx.doi.org/10.1002/chem.201704102>

Supported by
ACES

WILEY-VCH

Generation of Stable Ruthenium(IV)–Ketimido Complexes via Oxidative Addition of Oxime Esters to Ruthenium(II): Reactivity Studies Based on Electronic Properties of the Ru–N Bond

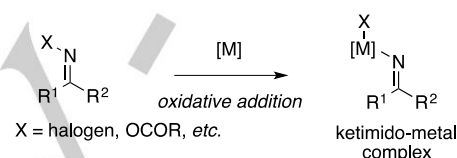
Takuya Shimbayashi, Kazuhiro Okamoto,* and Kouichi Ohe*^[a]

Abstract: The reaction of an oxime ester with $\text{RuX}_2(\text{PPh}_3)_3$ proceeded smoothly at room temperature to afford a stable Ru(IV)–ketimido complex as an oxidative adduct. The structure of the complex was unambiguously determined by X-ray crystallographic analysis, which showed an almost linear Ru–N–C array. The electronic properties of the nitrogen atom were estimated by density functional theory (DFT) calculations, and results suggested the double-bond character of the Ru–N bond. Kinetic studies combined with consideration of the substituent effect on the oxime ester led to proposing the reaction mechanism involving oxidative addition, which could proceed via *N,O*-chelate coordination to the Ru center prior to N–O bond cleavage. The obtained Ru–ketimido complex could be transformed into a ruthenacycle by C–H activation via the concerted metalation–deprotonation mechanism in dichloromethane/methanol mixed solvent. The Ru–ketimido complex exhibited another reactivity with a tethered alkyne or alkene moiety to undergo chloroamination of unsaturated C–C bonds, followed by C–H activation, resulting in the formation of an isolated ruthenacycle. Considering the LUMO of an isolated Ru–ketimido complex, the chloroamination should proceed via a synchronous 1,3-dipolar cycloaddition-type mechanism. Insight into the character and reactivity of Ru–ketimido complexes will be helpful for developments in the catalytic transformation of oxime esters.

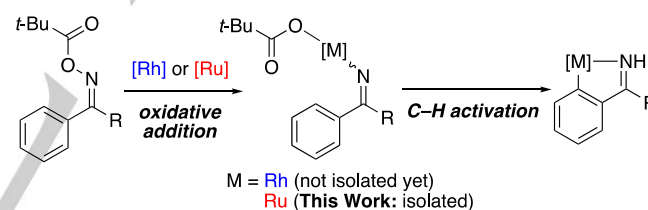
Introduction

Transition-metal-catalyzed processes involving N–O bond cleavage of oxime derivatives have recently been of interest due to their synthetic utility, especially for the efficient synthesis of *N*-heterocyclic compounds.¹ Many examples of such reactions have been reported since the pioneering work of Narasaka on a Pd-catalyzed intramolecular amino-Heck-type reaction.² Metal–ketimido complexes³ are considered key intermediates that can undergo 1,2-insertion to C–C unsaturated bonds⁴ or N–C reductive elimination from high-valent metal complexes⁵ to afford nitrogen-containing heterocycles involving a $\text{N}(\text{sp}^2)\text{--C}$ bond.⁶ However, mechanistic studies based on isolation of the ketimido complexes that are generated by oxidative addition of the oxime derivatives to low-valent metal species ($\text{M} = \text{Ti},^{7\text{a}} \text{Re},^{7\text{b}} \text{Os}^{7\text{c}},$

Pd^{d}) (Scheme 1) are still relatively scarce compared with the well-documented access to the ketimido complexes by stoichiometric reactions such as nucleophilic attack to metal–nitrile complexes ($\text{M} = \text{W},^{9\text{a,b}} \text{Re},^{9\text{c}} \text{Ru}^{9\text{d}}$), migratory insertion of M–R to nitrile^{10a} ($\text{M} = \text{Th},^{10\text{b}} \text{U},^{10\text{b}} \text{Ti},^{10\text{c,d}} \text{Zr},^{10\text{e}} \text{W},^{10\text{f}} \text{Fe},^{10\text{g}} \text{Rh}^{10\text{h}}$), and deprotonation–metalation starting from ketimines $\text{H–N=CRR}'$ ($\text{M} = \text{Zr},^{11\text{a}} \text{Cr},^{11\text{b}} \text{Mo},^{11\text{b}} \text{Fe}^{11\text{c}}$).¹² Therefore, a better understanding of the inherent nature of ketimido complexes prepared from oxime derivatives is significant for further developments in efficient catalytic reactions of oxime derivatives.



Scheme 1. Oxidative addition of oxime derivatives giving ketimido-metal complexes.



Scheme 2. Rh- or Ru-mediated oxidative cleavage of oxime esters.

During our concurrent studies on the transition-metal-catalyzed transformation of cyclic oxime esters involving the oxidative addition of a N–O bond to low-valent metal species,¹³ we found interesting reactivity of oxime esters with Rh(I) species that resulted in the formation of rhodacycles via oxidative addition followed by C–H activation (Scheme 2; $\text{M} = \text{Rh}$).¹⁴ The Rh(III)–ketimido complexes were assumed to have a bent C–N–Rh structure because they could not be isolated or observed due to the fast C–H activation.

Here, we report on a new type of Ru(IV)–ketimido complexes having a linear Ru–N–C array formed via the oxidative addition of oxime esters to Ru(II) precursors (Scheme 2; $\text{M} = \text{Ru}$). X-ray crystallographic analysis and density functional theory (DFT) calculations revealed the electronic properties, orbital interactions, and bonding characters of the ketimido complexes. The effect of the substituents on the aromatic rings of the oxime esters provides a deeper mechanistic insight into the oxidative addition. We found that ketimido complexes further underwent intramolecular C–H activation and haloamination of the internal unsaturated C–C bonds to afford new ruthenacycles under ambient conditions.

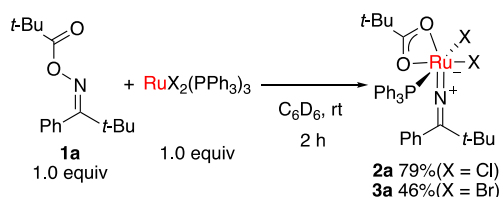
[a] Takuya Shimbayashi, Dr. Kazuhiro Okamoto, and Prof., Dr. Kouichi Ohe
Department of Energy and Hydrocarbon Chemistry, Graduate School of Engineering, Kyoto University
Nishikyo-ku, Kyoto 615-8510, Japan
E-mail: kokamoto@scl.kyoto-u.ac.jp; ohe@scl.kyoto-u.ac.jp

Supporting information for this article is given via a link at the end of the document.

Results and Discussion

Isolation of Ru–ketimido complexes

A stoichiometric reaction of oxime ester **1a** with $\text{RuCl}_2(\text{PPh}_3)_3$ in C_6D_6 at room temperature afforded 79% yield of imine complex **2a** as a green precipitate via oxidative addition (Scheme 3). The reaction of **1a** with the bromo analogue $\text{RuBr}_2(\text{PPh}_3)_3$ similarly afforded complex **3a** as a brown precipitate. Fine crystals of **2a** and **3a**, obtained by recrystallization from dichloromethane/hexane or benzene/hexane, were subjected to X-ray crystallographic analysis.¹⁵ Results clearly showed that a pivalate ligand coordinated to the Ru(IV) centers in η^2 fashion. The Ru–N bond in complex **2a** is 1.790 Å in length, which is similar to the bond length in the congener Os–ketimido complex (Os–N bond: 1.777 Å).^{7c} The length of the Ru–N bond is much shorter than the bond in second-row late-transition-metal–ketimido complexes (Rh–N bond: 2.039 Å, Pd–N bond: 1.999 Å),^{8a,12h} which implies stronger interaction between the nitrogen atom and the Ru center. The observed Ru–N–C1 angles of 169° (for **2a**) and 173° (for **3a**) indicated that both nitrogen atoms of these complexes have *sp* hybridization (Figure 1). This is the first example of mononuclear Ru–ketimido complexes having an almost linear Ru–N–C array confirmed by X-ray crystallographic analysis.^{16,17} Compared with the bent structure of ketimido complexes composed of second-row late transition metals such as Rh and Pd,^{8a,12h} the obvious structural difference from the Ru–ketimido complexes is of interest.



Scheme 3. Isolation of oxidative adducts **2a** and **3a**.

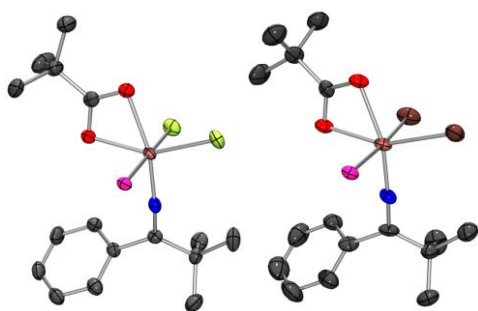


Figure 1. ORTEP illustrations of **2a** (left) and **3a** (right). Hydrogen atoms and phenyl groups on phosphorus atoms are omitted for clarity. Selected bond lengths [Å] and angles [°] for **2a**: Ru–N 1.790(4), N–C1 1.254(6), Ru–Cl1 2.297(1), Ru–Cl2 2.436(1), Ru–P 2.329(1), Ru–O1 2.123(3), Ru–O2 2.090(3), Ru–N–C1 168.6(4); and for **3a**: Ru–N 1.786(6), N–C1 1.273(9), Ru–Br1 2.440(1), Ru–Br2 2.555(1), Ru–P 2.334(2), Ru–O1 2.131(5), Ru–O2 2.086(4), Ru–N–C1 172.9(5).

Electronic properties of complex **2a** were estimated by DFT calculations using the B3LYP functional and LANL2DZ/6-31G(d,p) basis sets. The HOMO mainly contains the Ru–Cl2 antibonding orbital in which the orbital coefficients of the chlorine

atom are largest. This calculation is consistent with the elongated Ru–Cl2 bond compared with the Ru–Cl1 bond. In contrast, the LUMO mainly contains an antibonding orbital on the N–Ru–C1 three-atom unit (Figure 2). Hence this unit might undergo synchronous cycloaddition with nucleophiles rather than electrophiles. Moreover, NBO analysis supports the existence of the double-bond character of the Ru–N bond (Table 1), which is consistent with the relatively shorter Ru–N bond (bond length; 1.79 Å) as well as the linear array of the Ru–N–C1 structure around the nitrogen atom (bond angle; 173°). The *sp* hybridization of the nitrogen atom is what distinguishes it from the other late transition metals such as Pd and Rh.

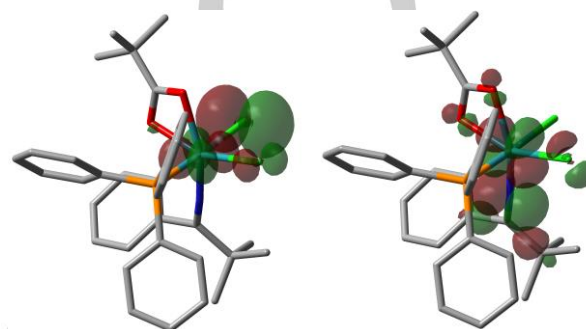


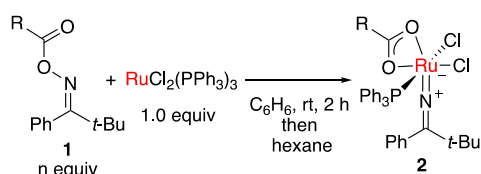
Figure 2. Illustration of HOMO (left) and LUMO (right) of **2a**. Calculation by B3LYP/LANL2DZ (for Ru) and 6-31G(d,p) (for other atoms). Isovalue is 0.045.

Table 1. NBO analysis of **2a**.

Type	Bond	Coefficient	Occupancy
BD	Ru–N	0.5113 Ru, 0.8594 N	1.93
BD	Ru–N	0.6807 Ru, 0.7326 N	1.87

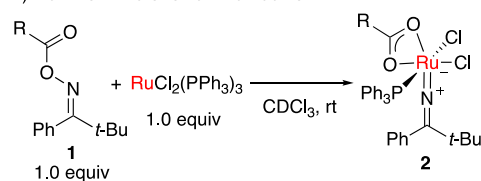
Effect of substituents on the reaction rate of oxidative addition

Steric hindrance of the *t*-Bu group on the ester moiety in **1** enabled easy isolation of the oxidative adducts due to stability and low solubility in benzene. When oxime esters with other substituents such as an isopropyl and ethyl group on the ester moiety were used, oxidative adducts **2b** and **2c** also formed, but no precipitates were observed. By adding hexane to the reaction mixture after 2 h, complexes **2b** and **2c** were successfully obtained as a green precipitate (Scheme 4a). Substituents on the carboxylate moiety did not significantly affect the structural properties of the Ru–ketimido complex.¹⁸ However, a variety of carboxylates had influence on the reaction rate of the oxidative addition. The rate constants became markedly smaller when the substituent was a less hindered isopropyl or ethyl group (Scheme 4b). These results imply a relationship between conformations of the oxime ester and the mechanism of oxidative addition. When the substituent on the ester moiety is the bulky *t*-Bu group, the oxime ester favors a conformation where the *t*-Bu group is far from the ketimine moiety. Such conformation can readily interact with the Ru(II) complex by *N,O*-chelation (Scheme 4c).

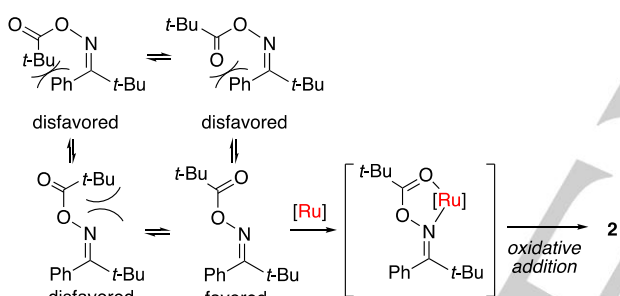
a) Isolation of oxidative adduct **2**.

entry	oxime ester	R	n	yield(%)
1	1a	<i>t</i> -Bu	1.1	87%
2	1b	<i>i</i> -Pr	2.5	93%
3	1c	Et	2.5	76%

b) Reaction rate of oxidative addition.



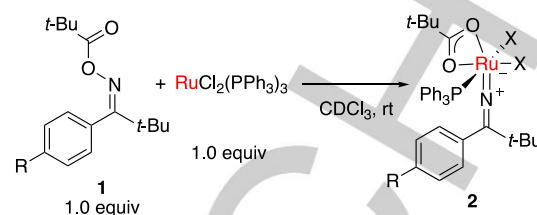
entry	oxime ester	R	k (mol·L ⁻¹ ·sec ⁻¹)
1	1a	<i>t</i> -Bu	0.155
2	1b	<i>i</i> -Pr	0.0878
3	1c	Et	0.0632

c) Conformations of oxime ester **1a**.

Scheme 4. a) Ruthenium-ketimido complexes with various carboxylate ligands. b) Substituent effect on the rate of oxidative addition. c) Conformational consideration on the mechanism for oxidative addition

To clarify the electronic effect of substituents on the reaction rate of oxidative addition, we employed various oxime esters **1** bearing substituents at the *para* position of the aromatic ring. The reaction rates observed in the oxidative addition to afford ketimido complexes **2** were very different, depending on the electronic nature of the *para* substituents (Scheme 5).¹⁸ When oxime esters having an electron-donating group such as NMe₂ and OMe were used, the rate constant *k* became lower than that of oxime **1a** (R = H). In contrast, a larger rate constant *k* was observed in an oxime ester having a nitro group as the strong electron-withdrawing group. A chloro substituent gave a marginal difference in the reaction rate compared with H substitution. Correlation of Hammett σ and *k* values provides linear fit with a ρ value of +0.194 calculated from its slope (Figure 3). This positive ρ value is rather small compared with the usual oxidative addition step using Pd(0) and aryl halides. The oxidative addition of N–O bonds to Ru(II) may indeed be triggered by nucleophilic attack of the Ru(II) center to the nitrogen atom. Simultaneously, the N–O bond may also be activated by the Lewis acidic effect of the Ru center toward an

oxygen atom, which may contribute to a lower ρ value. Overall, the oxidative addition would proceed through the *N,O*-chelating transition state that bears the slightly nucleophilic Ru(II) center (Scheme 4c).



R = NMe₂ (**1d**), OMe (**1e**), H (**1a**), Cl (**1f**), NO₂ (**1g**)

Scheme 5. Electronic influence on the reaction rate.

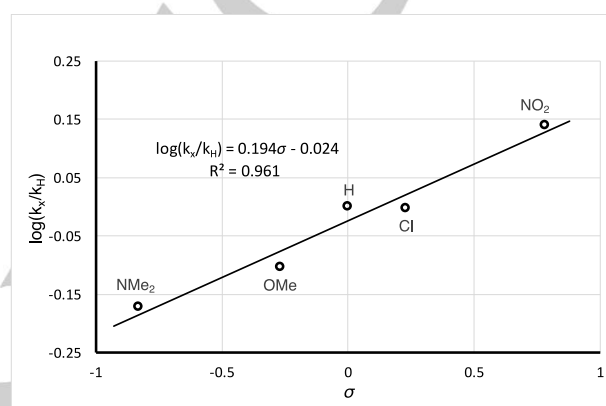
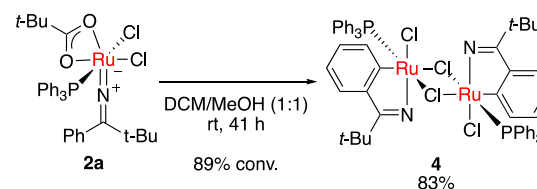


Figure 3. Hammett plot from reaction of **1** with RuCl₂(PPh₃)₃. Calculated ρ value is 0.194.

Formation of ruthenacycle by C–H activation

During our investigations into the reactivity of ketimido complex **2a**, we found that **2a** reacted in a 1:1 mixture of dichloromethane/methanol at room temperature to afford the chloro-bridged ruthenacycle dimer **4** quantitatively (Scheme 6). The crystal structure of **4**, obtained by recrystallization from dichloromethane/hexane, was successfully determined by X-ray diffraction analysis (Figure 4).¹⁹ Due to the long distance between the Ru center and the aromatic *ortho*-C(*sp*²)-H bond of a ketimine moiety, linear complex **2a** changes to bent ketimido complex **2a'** prior to C–H activation (Scheme 7). We presume that complex **2a'** undergoes intramolecular C–H activation via the concerted metalation–deprotonation (CMD) mechanism to form a Ru(IV) ruthenacycle **A**. Dimerization, followed by reduction with methanol, then leads to the formation of Ru(III) dimeric complex **4** as a paramagnetic complex.²⁰



Scheme 6. Formation of a ruthenacycle via C–H activation.

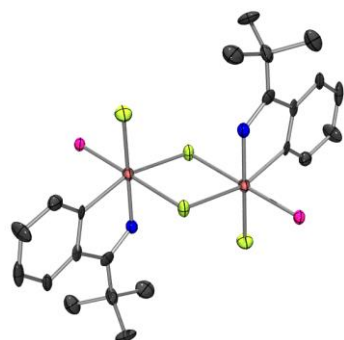
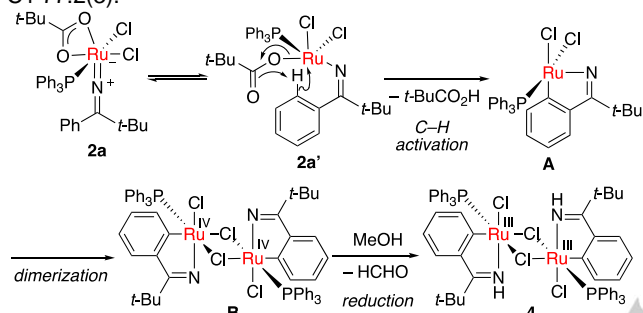


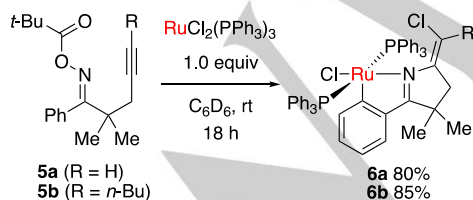
Figure 4. ORTEP illustration of **4**. Hydrogen atoms and phenyl groups on phosphorus atoms are omitted for clarity. Selected bond lengths [Å] and angles [°] for **4**: Ru–N 2.051(6), N–C2 1.320(1), Ru–C1 2.037(7), Ru–P 2.285(3), Ru–Cl1 2.349(2), Ru–Cl2 2.481(2), Ru–Cl2' 2.488(3), Ru–N–C2 120.8(5), N–Ru–C1 77.2(3).



Scheme 7. Plausible mechanism for the formation of complex **4**.

Ru-mediated tandem reaction of oxime esters bearing a C–C multiple bond

Studies on the reactivity of Ru–ketimido complexes toward unsaturated molecules such as alkenes and alkynes are of interest, especially in organic synthesis.²¹ The stoichiometric reaction of alkyne-tethered oxime ester **5** with $\text{RuCl}_2(\text{PPh}_3)_3$ in C_6D_6 at room temperature proceeded smoothly within 18 h, affording cyclic Ru(II) complex **6** in high yield (Scheme 8). X-ray diffraction analysis of complexes **6a** and **6b** clearly demonstrated the *cis* geometry of the nitrogen and chlorine atoms in the olefinic moiety (Figure 5), which indicates the formation of these complexes via *syn* chloroamination.²² Both complexes **6a** and **6b** have a vacant coordination site at the *trans* position to the aromatic ligand. Distribution of the LUMO in ketimido complex **2a** as shown in Figure 2 predictively suggests the 1,3-dipolar nature of the N–Ru–Cl unit.



Scheme 8. Intramolecular chloroamination of alkynes.

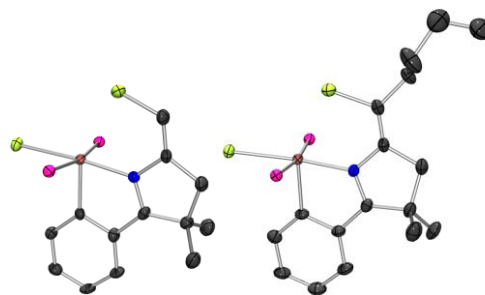
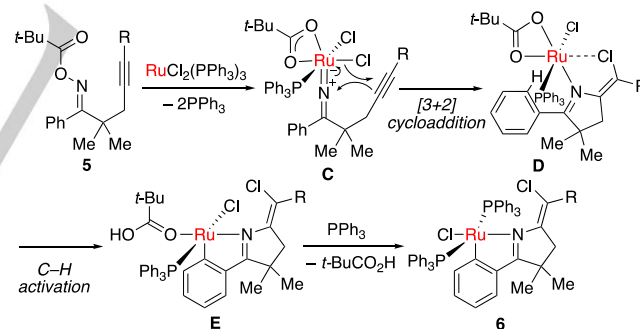


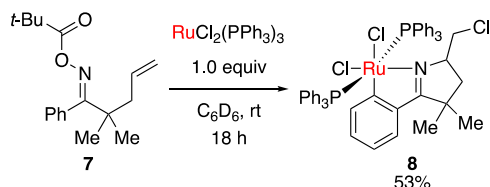
Figure 5. ORTEP illustration of ruthenacycle **6a** (left) and **6b** (right). Hydrogen atoms and phenyl groups on phosphorus atoms are omitted for clarity. Selected bond lengths [Å] and angles [°] for **6a**: Ru–N 2.007(3), N–C2 1.324(6), Ru–C1 1.989(4), Ru–P1 2.362(1), Ru–P2 2.350(1), Ru–Cl1 2.446(1), Ru–Cl2 2.857(1), Ru–N–C2 118.9(3), N–Ru–C1 78.9(1); and for **6b**: Ru–N 2.003(3), N–C2 1.310(5), Ru–C1 2.017(4), Ru–P1 2.375(1), Ru–P2 2.344(1), Ru–Cl1 2.452(1), Ru–Cl2 2.747(1), Ru–N–C2 119.9(3), N–Ru–C1 78.2(2).

Based on the above observations, a plausible mechanism for the formation of ruthenacycle **6** is shown in Scheme 9. First, a Ru(II) species undergoes the oxidative addition of oxime ester **5** to generate a Ru(IV)–ketimido complex **C** as an intermediate. Then, the 1,3-dipolar type of cycloaddition of the alkyne moiety with the Ru–N–Cl unit might occur synchronously to afford the *syn*-chloroamination product **D**. Then intramolecular C–H activation via the CMD mechanism would occur more favorably in intermediate **D** than in the prior complex **C** due to the proximity of the C–H bond to the Ru center. Finally, the coordination of another PPh_3 to complex **E**, with the release of pivalic acid, affords ruthenacycle complex **6**.



Scheme 9. Plausible mechanism for the formation of complex **6**.

Similarly, alkene-tethered oxime ester **7** also reacted smoothly with the Ru(II) complex to afford ruthenacycle **8** in moderate yield (Scheme 10). X-ray diffraction analysis of a single crystal of ruthenacycle **8** obtained by slow evaporation from dichloromethane/benzene demonstrates that, in contrast to ruthenacycle **6**, this complex has a Ru(III) center (Figure 6).²³ Complex **8** would also be formed via chloroamination of the alkene moiety in **7** followed by C–H activation. Compared with Ru(II) complex **6**, Ru(III) complex **8** has one more chloro ligand at the *trans* position to the *ipso* carbon atom of the aryl group, which is vacant in complex **6**. Complex **8** might be formed via comproportionation between Ru(IV) and Ru(II) owing to the vacant coordination site accessible for the chlorine atom.



Scheme 10. Intramolecular chloroamination of an alkene.



Figure 6. ORTEP illustration of ruthenacycle **8**. Hydrogen atoms and phenyl groups on phosphorus atoms are omitted for clarity. Selected bond lengths [Å] and angles [°]: Ru–N 2.100(3), N–C2 1.303(5), Ru–C1 2.056(3), Ru–P1 2.405(1), Ru–P2 2.399(1), Ru–Cl1 2.332(1), Ru–Cl2 2.463(1), Ru–N–C2 117.7(2), N–Ru–C1 76.8(1)

Conclusions

A new type of Ru(IV)–ketimido complexes has been obtained by the oxidative addition of oxime esters to Ru(II). X-ray crystallographic analysis unambiguously revealed their linear Ru–ketimido structure. DFT calculations also supported the *sp* hybridization character of the nitrogen atoms and the double-bond character of the Ru–N bond, reflecting the linear Ru–N–C structure. The ketimido complexes readily underwent CMD-type C–H activation to form stable ruthenacycle complexes. Furthermore, the ketimido complexes underwent intramolecular *syn* chloroamination with an alkyne or an alkene moiety, as predicted by DFT calculations. The observations and calculations of the electronic properties of Ru–ketimido complexes, especially concerning Ru–N bonding, should be helpful for further investigations of catalytic transformation involving metal–ketimido intermediates.

Acknowledgement

This study has been financially supported by Grant-in-aid for JSPS Research Fellow (T.S.) (Grant No. 17J09627) and JSPS KAKENHI (a Scientific Research (C); Grant No. 17K05861).

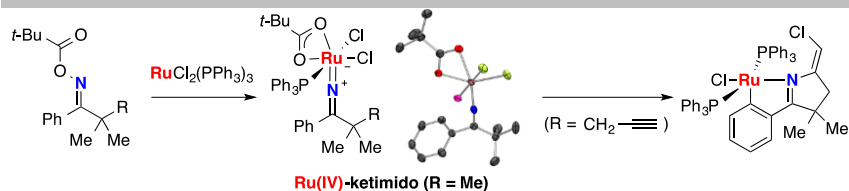
Keywords: Ruthenium • N ligands • Coordination modes • C–H activation • Amination

- For reviews, see: a) M. Kitamura, K. Narasaka, *Chem. Rec.* **2002**, *2*, 268; b) K. Narasaka, M. Kitamura, *Eur. J. Org. Chem.* **2005**, 4505; c) H. Huang, X. Ji, W. Wu, H. Jiang, *Chem. Soc. Rev.* **2015**, *44*, 1155; d) H. Huang, J. Cai, G.-J. Deng, *Org. Biomol. Chem.* **2016**, *14*, 1519.
- H. Tsutsui, K. Narasaka, *Chem. Lett.* **1999**, 28, 45.
- For a review, see: M. J. Ferreira, A. M. Martins, *Coord. Chem. Rev.* **2006**, *250*, 118.
- R. Castarlenas, M. A. Esteruelas, E. Oñate, *Organometallics* **2001**, *20*, 2294.
- G. Mann, J. F. Hartwig, M. S. Driver, C. Fernández-Rivas, *J. Am. Chem. Soc.* **1998**, *120*, 827.
- For a review, see: R. He, Z.-T. Huang, Q.-Y. Zheng, C. Wang, *Tetrahedron Lett.* **2014**, *55*, 5705.
- a) A. Tillack, P. Arndt, A. Spannenberg, R. Kempe, U. Rosenthal, *Z. Anorg. Allg. Chem.* **1998**, *624*, 737; b) C. M. P. Ferreira, M. F. C. Guedes da Silva, V. Y. Kukushkin, J. J. R. Fraústo, A. J. L. Pombeiro, *J. Chem. Soc., Dalton Trans.* **1998**, 325; c) R. Castarlenas, M. A. Esteruelas, E. Gutiérrez-Puebla, Y. Jean, A. Lledós, M. Martín, E. Oñate, J. Tomàs, *Organometallics* **2000**, *19*, 3100.
- a) Y. Tan, J. F. Hartwig, *J. Am. Chem. Soc.* **2010**, *132*, 3676; b) W. P. Hong, A. V. Iosub, S. S. Stahl, *J. Am. Chem. Soc.* **2013**, *135*, 13664.
- a) S. G. Feng, P. S. White, J. L. Templeton, *J. Am. Chem. Soc.* **1994**, *116*, 8613; b) N. J. Vogeley, J. L. Templeton, *Polyhedron* **2004**, *23*, 311; c) A. C. Hillier, T. Fox, H. W. Schmalke, H. Berke, *J. Organomet. Chem.* **2003**, *669*, 14; d) W. K. Fung, X. Huang, M. L. Man, S. M. Ng, M. Y. Hung, Z. Lin, C. P. Lau, *J. Am. Chem. Soc.* **2003**, *125*, 11539.
- For a review, see: a) S. Kobayashi, M. Sugiura, U. Schneider, R. Matsubara, J. Fossey, Y. Yamashita, In *Comprehensive Organometallic Chemistry III*; R. H. Crabtree, D. M. P. Mingos, Eds.; Elsevier: Oxford, 2007; Vol. 10, pp 403-491; b) K. C. Jantunen, C. J. Burns, I. Castro-Rodriguez, R. E. Da Re, J. T. Golden, D. E. Morris, B. L. Scott, F. L. Taw, J. L. Kiplinger, *Organometallics* **2004**, *23*, 4682; c) M. Bochmann, L. M. Wilson, M. B. Hursthouse, M. Motevalli, *Organometallics* **1988**, *7*, 1148; d) N. A. Petasis, D.-K. Fu, *Organometallics* **1993**, *12*, 3776; e) S. K. Podiyanchari, R. Fröhlich, C. G. Daniliuc, J. L. Petersen, C. Mück-Lichtenfeld, G. Kehr, G. Erker, *Angew. Chem. Int. Ed.* **2012**, *51*, 8830; f) Q. X. Dai, H. Seino, Y. Mizobe, *Organometallics* **2012**, *31*, 4933; g) A. Klose, E. Solari, C. Floriani, A. Chiesi-Villa, C. Rizzoli, N. Re, *J. Am. Chem. Soc.* **1994**, *116*, 9123; h) P. Zhao, J. F. Hartwig, *Organometallics* **2008**, *27*, 4749.
- a) G. Erker, W. Frömberg, C. Krüger, E. Raabe, *J. Am. Chem. Soc.* **1988**, *110*, 2400; b) R. A. D. Soriaga, J. M. Nguyen, T. A. Albright, D. M. Hoffman, *J. Am. Chem. Soc.* **2010**, *132*, 18014; c) R. A. Lewis, G. Wu, T. W. Hayton, *J. Am. Chem. Soc.* **2010**, *132*, 12815.
- Other routes to ketimido complex, see a) E. A. Maatta, Y. Du, *J. Am. Chem. Soc.* **1988**, *110*, 8249; b) T. Daniel, M. Müller, H. Werner, *Inorg. Chem.* **1991**, *30*, 3120; c) S. N. Brown, *Inorg. Chem.* **2000**, *39*, 378; d) Y. Tanabe, H. Seino, Y. Ishii, M. Hidai, *J. Am. Chem. Soc.* **2000**, *122*, 1690; e) S. M. P. R. M. Cunha, M. F. C. Guedes da Silva, A. J. L. Pombeiro, *J. Chem. Soc., Dalton Trans.* **2002**, 1791; f) M. F. C. Guedes da Silva, J. J. R. Fraústo da Silva, A. J. L. Pombeiro, *Inorg. Chem.* **2002**, *41*, 219; g) A. R. Cowley, J. R. Dilworth, A. K. Nairn, A. J. Robbie, *Dalton Trans.* **2005**, 680; h) P. Zhao, J. F. Hartwig, *J. Am. Chem. Soc.* **2005**, *127*, 11618; i) E. Lu, Q. Zhou, Y. Li, J. Chu, Y. Chen, X. Leng, J. Sun, *Chem. Commun.* **2012**, *48*, 3403.
- a) K. Okamoto, T. Oda, S. Kohigashi, K. Ohe, *Angew. Chem. Int. Ed.* **2011**, *50*, 11470; b) K. Okamoto, T. Shimabayashi, E. Tamura, K. Ohe, *Chem.—Eur. J.* **2014**, *20*, 1490; c) T. Shimabayashi, K. Okamoto, K. Ohe, *Synlett* **2014**, *25*, 1916; d)

- K. Okamoto, T. Shimbayashi, M. Yoshida, A. Nanya, K. Ohe, *Angew. Chem. Int. Ed.* **2016**, *55*, 7199; e) K. Okamoto, K. Sasakura, T. Shimbayashi, K. Ohe, *Chem. Lett.* **2016**, *45*, 988.
- (14) T. Shimbayashi, K. Okamoto, K. Ohe, *Organometallics* **2016**, *35*, 2026.
- (15) CCDC 1574833 (**2a**) and 1574836 (**3a**) contain the supplementary crystallographic data. These data can be obtained free of charge from The Cambridge Crystallographic Data Centre.
- (16) Ru-aza-allenylidene, Ru₃ cluster and Ru₂ cluster were reported. a) M. I. Bruce, M. A. Buntine, K. Costuas, B. G. Ellis, J.-F. Halet, P. J. Low, B. W. Skelton, A. H. White, *J. Organomet. Chem.* **2004**, *689*, 3308; b) C. Bois, J. A. Cabeza, R. J. Franco, V. Riera, E. Saborit, *J. Organomet. Chem.* **1998**, *564*, 201; c) J. A. Cabeza, I. del Río, F. Grepioni, M. Moreno, V. Riera, M. Suárez, *Organometallics* **2001**, *20*, 4190.
- (17) Congener Os-ketimido complexes were reported: a) H. Werner, W. Knaup, M. Dziallas, *Angew. Chem. Int. Ed.* **1987**, *26*, 248; b) R. Castarlenas, M. A. Esteruelas, E. Gutiérrez-Puebla, E. Oñate, *Organometallics* **2001**, *20*, 1545; c) R. Castarlenas, M. A. Esteruelas, E. Oñate, *Organometallics* **2001**, *20*, 3283; d) R. Castarlenas, M. A. Esteruelas, Y. Jean, A. Lledós, E. Oñate, J. Tomás, *Eur. J. Inorg. Chem.* **2001**, 2871; e) J. Chen, Z.-A. Huang, Z. Lu, H. Zhang, H. Xia, *Chem.—Eur. J.* **2016**, *22*, 5363.
- (18) See the Supporting Information. CCDC 1574834 (**2b**), 1574835 (**2c**) and 1574841 (**2e**).
- (19) CCDC 1574839 (**4**).
- (20) Complex **2a** did not undergo ruthenacycle formation in the absence of methanol, which suggests that methanol may assist facile isomerization from linear ketimido complex to bent ketimido complex probably due to protic interaction. Similar effect was reported on another ruthenium system but the reason is still unclear. C. Bohanna, M. A. Esteruelas, A. M. López, L. A. Oro, *J. Organomet. Chem.* **1996**, *526*, 73.
- (21) Intermolecular cycloaddition of ruthenacycle **3a** with terminal alkynes also afforded isoquinoline as cycloadduct, albeit in low yield. See Supporting Information for details.
- (22) CCDC 1574837 (**6a**) and 1574840 (**6b**).
- (23) CCDC 1574838 (**8**).

Entry for the Table of Contents (Please choose one layout)

FULL PAPER



It's clearly linear: Stable ruthenium(IV)-ketimido complexes were obtained via oxidative addition of oxime esters to ruthenium(II). X-ray diffraction revealed their linear Ru–N–C arrays. DFT calculation supports the electronic nature of Ru–N bond. The ketimido complex could be an intermediate for chloroamination of an alkyne or alkene.

T. Shimbayashi, K. Okamoto,* K. Ohe*

Page No. – Page No.

Generation of Stable Ruthenium(IV)–Ketimido Complexes via Oxidative Addition of Oxime Esters to Ruthenium(II): Reactivity Studies Based on Electronic Properties of the Ru–N Bond